Proc. Natl. Acad. Sci. USA
Vol. 92, pp. 1441–1445, February 1995
Neurobiology

Glycinergic synaptic currents in Golgi cells of the rat cerebellum

STÉPHANE DIEUDONNÉ

Laboratoire de Neurobiologie, Ecole Normale Supérieure, 46 rue d'Ulm, 75005 Paris, France

Communicated by Clay M. Armstrong, University of Pennsylvania School of Medicine, Philadelphia, PA, October 31, 1994 (received for review April 10, 1994)

ABSTRACT **Recordings were made from Golgi cells in slices from rat cerebellar cortex using whole-cell and outside-out configurations of the patch-clamp technique. Exogenous glycine and γ-aminobutyric acid (GABA) both activated chloride currents, which could be differentially blocked by strychnine and SR95531, respectively. Inhibitory synaptic currents occurred spontaneously in all Golgi cells. Some were blocked by strychnine while the others were blocked by SR95531. The single channel events occurring during the decay of these two types of inhibitory postsynaptic currents had different amplitudes, which matched the main conductance states of the channels gated by glycine and GABA in outside-out patches. It was concluded that Golgi cells receive both glycinergic and GABAergic synaptic inputs.**

γ-Aminobutyric acid (GABA) and glycine are the two major inhibitory transmitters in the vertebrate central nervous system. GABA is considered to be ubiquitous, and its involvement in synaptic transmission has been demonstrated at numerous synapses from the spinal cord to the cerebral cortex. In contrast, the role of glycine as an inhibitory neurotransmitter has often been considered as limited to a few specific structures: the spinal cord, where glycinergic synaptic currents coexist with GABAergic synaptic currents (1, 2), the brain stem, where glycinergic synaptic currents have been well described in some large neurons (3, 4), and the retina (5). The notion that glycinergic inhibitory synaptic transmission is absent from other structures rostral to the spinal cord is based on the observation that the density of glycine receptors, assessed by the number of high-affinity strychnine binding sites, decreases markedly as one proceeds from the spinal cord toward more anterior structures (6).

However, many data suggest that glycine could be a transmitter in these structures. Immunohistochemical evidence indicates the presence of neurons with a high concentration of intracellular glycine in regions as diverse as the thalamus, the cerebellar cortex, the hippocampus, the striatum, and the cortex (7–9). The demonstration of powerful glycine uptake systems in the same structures provides a possible pathway for inactivation of synaptically released glycine (10). Glycine receptors have been detected by immunohistochemical methods (7, 11) in many regions of the brain (including the cerebellum), where strychnine binding sites had not been detected. After the cloning of several subunits of the glycine receptor, Northern blots have revealed that the corresponding mRNAs were transcribed in higher regions of the central nervous system (12, 13), and *in situ* hybridization has shown that the transcription of these subunits was temporally and spatially regulated throughout the brain (14). Finally, the existence of functional inhibitory glycine receptors is established by the fact that glycine-induced Cl^- currents have been recorded from neurons (either cultured or acutely isolated) originating from hypothalamus (15), hippocampus (16), olfactory bulb (17), and cerebral cortex (18), as well as from CA3 pyramidal neurons in rat hippocampal slices (19) and from granule cells in slices of the cerebellar cortex (20).

These data indicate that glycinergic inhibitory synapses may be widely distributed in the central nervous system. However, proof of the existence of glycinergic inhibitory postsynaptic currents (IPSCs) is missing in all the structures cited above where glycine-activated currents have been recorded, and the possibility remains that the glycine receptors detected in higher brain areas are largely located at extrasynaptic sites. Presented here is evidence for the existence of functional glycinergic inputs on Golgi cells of the rat cerebellar cortex.

METHODS

Slice Preparation. Cerebellar slices were obtained following the method originally described by Llinás and Sugimori (21) with slight modifications (22, 23). Male Wistar rats aged 10–25 days were used. Parasagittal slices, 160–200 μm thick, were cut from the cerebellar vermis.

Identification of Golgi Cells. The cell body of Golgi interneurons, located in the granular layer of the cerebellar cortex, had to be distinguished from the three other cell types present in this layer: granule cells, Lugaro interneurons, and glial cells. Granule cell somata, which represent the vast majority of the cell bodies in the granular layer, are much smaller (4–7 μm) than the somata of the Golgi cells (8–25 μm) (24). This difference was used as the main criterion to distinguish the two cell types. Additional differences appeared in the analysis of capacitive currents and of Na^+ current. In presumptive granule cells, capacitive currents followed a single exponential, with an estimated cell capacitance smaller than 4 pF. The capacitive current in presumptive Golgi cells was biexponential. A lower estimate of the capacitance of these cells, obtained by canceling the fast component of the capacitive current transient, yielded values of 6–88 pF. This scatter is in line with the large variation in the size of morphologically identified Golgi cells (24). Fast inactivating, tetrodotoxin-sensitive, inward currents elicited by depolarizing voltage jumps (from −70 mV to −40 mV) were observed both in large (presumably Golgi) and small (presumably granule) cells. However, they were on average 60 times larger in large cells than in small cells. It was also noted that small cells were not spontaneously active, whereas large cells often fired action potentials that could be recorded in the cell-attached configuration.

Lugaro interneurons have fusiform cell bodies located just under the Purkinje cell layer (24). To avoid mistaking these neurons for Golgi cells, cell bodies situated in the upper fifth of the granular layer were not considered in this study.

Cells with large membrane capacitance (>5 pF) that showed no spontaneous synaptic currents and small voltage-activated inward currents (<500 pA) were assumed to be glial cells.

Patch-Clamp Recording. All experiments were performed at room temperature. The recording chamber was continuously perfused with a saline solution containing 125 mM NaCl,

The publication costs of this article were defrayed in part by page charge payment. This article must therefore be hereby marked "*advertisement*" in accordance with 18 U.S.C. §1734 solely to indicate this fact.

Abbreviations: GABA, γ-aminobutyric acid; IPSC, inhibitory postsynaptic current; EPSC, excitatory postsynaptic current; CNQX, 6-cyano-7-nitroquinoxaline-2,3-dione.

2.5 mM KCl, 2 mM $CaCl_2$, 1 mM $MgCl_2$, 1.25 mM NaH_2PO_4, 26 mM $NaHCO_3$, and 25 mM glucose, bubbled with 95% O_2/5% CO_2 (pH 7.4). The preparation was observed with a ×40 water-immersion objective. Pipettes for whole-cell recording had a resistance of 1–5 MΩ. The capacitive current of Golgi cells was well described by the sum of two exponential functions with time constants of 90 ± 10 μs and 540 ± 60 μs (n = 7). The fast component was canceled, and the access resistance was then compensated (23). No compensation was performed in the cells where a low noise level was required to detect single channel closings in the synaptic events. In these small cells (capacitance <10 pF), the input resistance ranged from 0.5 to 1 GΩ. To form outside-out patches, pipettes of 10- to 20-MΩ resistance were used. The usual composition of the pipette solution was 155 mM CsCl, 5 mM $MgCl_2$, 0.1 mM $CaCl_2$, 1 mM EGTA, 10 mM Hepes, 4 mM Na_2ATP_1, 0.4 mM Na_2GTP (pH adjusted to 7.3–7.4 with CsOH or *N*-methyl-D-glucamine). For low internal chloride recordings, part of the CsCl was replaced by CsF, and the Ca^{2+} buffering capacity was raised to avoid the formation of CaF_2 complexes. This low chloride solution contained 20 mM CsCl, 130 mM CsF, 1 mM $MgCl_2$, 1 mM $CaCl_2$, 10 mM EGTA, 10 mM Hepes (pH adjusted to 7.3–7.4 with *N*-methyl-D-glucamine).

Drug Application. Agonists were bath-applied, and the agonist-induced currents were allowed to reach a reasonably stable level before one of the antagonists was added into the bathing solution. The amplitude of the desensitization observed at the beginning of the agonist application was very variable from cell to cell. This can be explained by the impossibility to clamp the concentration of agonist inside the slice. Low-affinity antagonists were removed during continuous agonist application to measure recovery. High-affinity antagonists were removed simultaneously with the agonist, because of the lack of stability of agonist-induced currents during the many minutes necessary for recovery.

For the construction of current–voltage relations, local perfusion was used to reduce the possibility of chloride reequilibration. A glass pipette (5- to 20-μm tip diameter) was filled with bath solution (containing 500 nM tetrodotoxin, 50 μM aminophosphonovaleric acid) to which 100 μM glycine was added and placed ≈100 μm away from the recorded cell. Pulses 100–600 ms long generated responses with a rise time under 1 s, which decayed within a few seconds. The same technique was used to apply agonists to outside-out patches.

Data Analysis. Records were usually filtered at 0.5–2 kHz and digitized off-line (sampling rate, 3–10 kHz). All data point histograms could not be used to analyze the channels underlying IPSCs, since these are composed of multiple channel openings which, combined with the multiple conductance states, prevented the appearance of regularly spaced peaks in the histogram. To use a single measurement protocol for IPSCs and patch data, long lasting (5 s to 1 min) applications of high agonist concentrations were used to activate simultaneously several channels in patches. Only upward current steps (reflecting channel closings or transition of an open channel to a smaller conductance state) occurring during drug-induced currents were measured, to permit comparison with the IPSC decay. These steps were measured using software kindly provided by S. Traynelis (Salk Institute of Biological Studies, La Jolla, CA). In this analysis, a current step was considered as valid when it was steep and when it was preceded and followed by more than 1 ms of steady current. Step size was measured between two manually adjustable horizontal cursors. To reduce contamination of the data by multistep closures, the analysis was restricted to the last 30 pA of the IPSC decay. Values are given as means ± SD.

RESULTS

Current–Voltage Relations of Glycine-Evoked Currents. Bath-applied glycine (30–300 μM) evoked currents larger than 100 pA in all the Golgi cells tested (n = 27). These currents were insensitive to tetrodotoxin, indicating that the glycine receptors were on the recorded cells. They were insensitive to aminophosphonovaleric acid, and therefore they did not result from coactivation of *N*-methyl-D-aspartate receptors by glycine and by endogenous glutamate. The glycine-activated channels studied in various neurons are highly permeable to Cl^- ions, poorly permeant to F^- ions, and display some outward rectification in physiological conditions (25). Similar properties were found in Golgi cells. Short pulses of glycine (100 μM) were pressure-applied to the cell, generating currents that developed over 1 s and decayed to baseline within a few seconds. The current–voltage relation for currents measured at the peak of the response displays outward rectification, whereas the Goldman–Hodgkin–Katz equation predicts a slight inward rectification for the ionic conditions used. The interpolated reversal potential is +8 mV, close to the Cl^- equilibrium potential (+6 mV). After partial replacement of internal Cl^- by F^- ($[Cl^-]_i$ = 24 mM), the reversal potential was shifted near to the new Cl^- equilibrium potential (−42 mV).

Pharmacological Characterization of Glycine-Evoked and GABA-Evoked Currents. Glycine- and GABA-induced responses were differentially sensitive to strychnine and to SR95531. Strychnine (300 nM) inhibited the response to glycine (30–50 μM) by 94% ± 1% (n = 5) (Fig. 1*A*). This is consistent with the reported K_i for strychnine, which falls in the range of 2–14 nM for most of the molecular isoforms of the glycine receptor (26). In contrast, $GABA_A$ currents were inhibited by only 12% ± 1% (n = 3) by 300 nM strychnine (Fig. 1*B*), and 10 μM strychnine was required to achieve a 70% ± 5% block (n = 3). GABA-activated currents were totally blocked by 30 μM SR95531. At this concentration, which is 180 times the reported IC_{50} of SR95531 for the $GABA_A$ currents (27), glycine-activated currents were only decreased by 38% ± 5% (n = 4) (Fig. 1*B*). Thus, glycine-activated currents have a different pharmacological profile than $GABA_A$ currents.

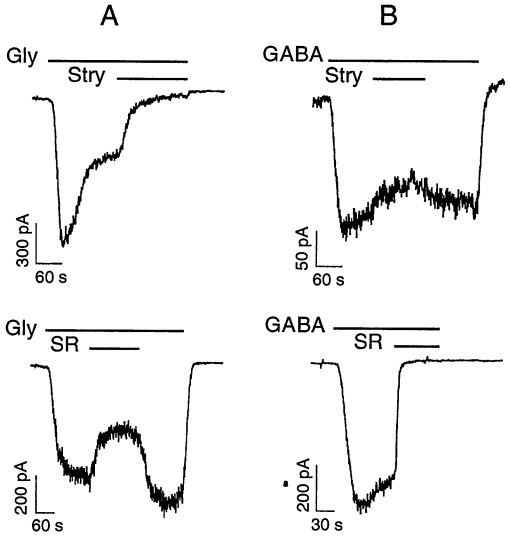

FIG. 1. Pharmacological profile of currents activated by glycine (Gly) and GABA. Glycine (50 μM) and GABA (10 μM) were bath-applied to Golgi cells (four experiments) clamped at V_H = −70 mV in symmetrical Cl^- concentration conditions. (*A*) Blocking effects of strychnine (Stry) and SR95531 on glycine-induced currents. In the upper trace the current is reduced by 93% by 300 nM strychnine. Recovery was nearly complete after 20 min of wash out (not shown). In the lower trace, the current is reduced by 44% by 30 μM SR95531, showing that SR95531 is not totally selective for GABA receptors. (*B*) Blocking effects of 300 nM strychnine (upper trace, 13% reduction) and 30 μM SR95531 (lower trace, total block) on GABA-induced currents.

Single-Channel Events Underlying Glycine and GABA-Evoked Currents. Glycine-induced single-channel openings had at least five amplitude levels. The two most frequently observed levels, which were present in all four patches analyzed, are illustrated in the upper trace of Fig. 2*A*. Their amplitudes correspond to chord conductances of 35 ± 2 pS and 47 ± 1 pS (n = 4) (Fig. 2*B*). These values are consistent with results in other cells (2, 25, 28, 29).

Selected records of GABA-activated channels are shown in Fig. 2*C*. The highest conductance level (25 ± 1 pS; n = 5) was predominant in all five patches recorded, although smaller conductance states (12 pS and 17 pS; Fig. 2*C*) were observed in four patches. Fig. 2*D* shows the amplitude distribution of upward current steps during long GABA applications. The histogram is fitted by two Gaussian functions, yielding mean conductances of 18 pS and 24 pS. The 25-pS conductance level represents about 75% ± 9% (n = 5) of the current steps. No opening corresponding to a conductance state larger than 25 pS was detected. Thus, the GABA-gated channels have a smaller preferred elementary conductance than the glycine-gated channels.

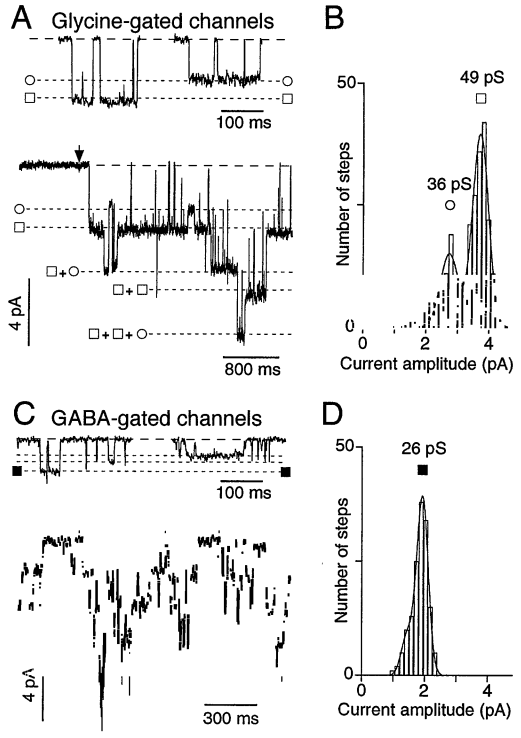

FIG. 2. GABA-gated and glycine-gated single-channel currents in outside-out patches excised from Golgi cells. In all experiments, the high Cl^- concentration pipette solution was used, and patches were voltage-clamped at V_H = −70 mV. Glycine (100 μM) and GABA (10 μM) were pressure-applied. (*A*) The upper traces display the two most frequent elementary current amplitudes of the glycine-activated channels, −2.7 pA (○) and −3.7 pA (□). The lower trace shows multiple channel openings during a prolonged application of glycine (starting at arrow). The current can be accounted for by the asynchronous openings and closings of three channels with elementary currents of −2.7 pA (○) and −3.8 pA (□). (*B*) Amplitude histogram of upward current steps occurring during 29 s of glycine application. The solid line is a fit of the data by two Gaussians with means of 2.7 pA and 3.75 pA, corresponding to chord conductances of 36 pS and 49 pS. (*C*) The upper traces display the three most frequent elementary current amplitudes of GABA-activated channels. The main amplitude level (−2 pA) is marked by filled squares. The other lines correspond to −1.5 pA and −1 pA. The lower trace shows multiple channel openings induced by a prolonged application of GABA. The dashed lines are separated by equal intervals of 2.0 pA, corresponding to a chord conductance of 26 pS. Note that GABA-gated channels spend most of their open time in this conductance state. (*D*) Amplitude histogram of upward current steps during a 11.5-s application of GABA. It is fitted by two Gaussians (solid line) of means 1.4 pA and 1.9 pA (chord conductances of 18 pS and 24 pS; the latter accounts for 80% of the steps).

Spontaneous Synaptic Activity in Golgi Cells. To test if the glycine-gated channels expressed by Golgi cells were involved in synaptic transmission, recordings of the spontaneous synaptic activity were obtained from Golgi cells perfused with the high Cl^- internal solution and clamped at −70 mV. Two types of synaptic currents were identified on the basis of their kinetic properties. Fast decaying synaptic currents (decaying to baseline within 5 ms), blocked by 6-cyano-7-nitroquinoxaline-2,3-dione (CNQX) at micromolar concentrations, were present in most (but not all) cells. They were interpreted as glutamatergic excitatory postsynaptic currents (EPSCs). Slowly decaying synaptic currents were recorded from all cells (n = 38). These currents persisted in the presence of CNQX (five cells) but were blocked by simultaneous application of strychnine (300 nM to 3 μM) and SR95531 (30 μM), suggesting that they result from the activation of either $GABA_A$ or glycine receptors. They will henceforth be called IPSCs.

These IPSCs were classified as glycinergic and GABAergic by taking advantage of the selective effects of strychnine (300 nM) and SR95531 (30 μM) on the currents induced by glycine and GABA, respectively. Fig. 3*A* and *B* illustrates a case where application of 30 μM SR95531 (in conjunction with CNQX) blocked many of the IPSCs but not all of them. When strychnine (300 nM) was applied to the slice (Fig. 3*C*), it blocked reversibly (Fig. 3*D*) the inhibitory activity persisting in the presence of SR95531. The amplitude and kinetics of SR95531-sensitive and SR95531-insensitive, strychnine-sensitive IPSCs were both variable. Variability from cell to cell as well as evolution during development of the cerebellum

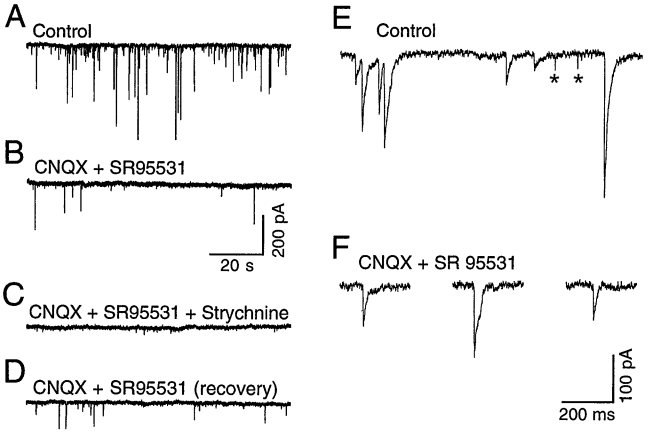

FIG. 3. Pharmacological profile of the spontaneous synaptic currents in Golgi cells. Spontaneous synaptic currents were recorded at −70 mV from a Golgi cell dialyzed with the high Cl^- pipette solution. (*A*) Spontaneous synaptic activity in control saline. The mean IPSC frequency was 2.1 Hz. (*B*) Effect of the combined application of a $GABA_A$ antagonist SR95531 (30 μM) and of the non-*N*-methyl-D-aspartate glutamate receptor antagonist CNQX (2 μM). The synaptic activity was not completely abolished by the two antagonists. The remaining IPSCs, which had a mean frequency of 0.2 Hz, persisted for more than 50 min. (*C*) IPSCs persisting in the presence of SR95531 and CNQX were blocked by strychnine (300 nM). (*D*) Reversal after strychnine wash out. (*E*) Display, on a faster time scale, of the control synaptic activity. Six slowly decaying IPSCs are followed by two rapidly decaying EPSCs (*). (*F*) Expanded display of some IPSCs persisting in the presence of CNQX and SR95531. In this cell, the decay of these IPSCs is similar to that of the control IPSCs (*E*). In *A–D*, the traces were digitalized at 1 kHz, and the maximum and minimum were plotted every 40 points. This method allows the conservation of the exact size of the events even though the final sampling rate is equivalent to 50 Hz. Sampling frequency in *E* and *F* was 5 kHz. The scales are the same for *A–D* and also for *E* and *F*.

Table 1. Inhibition of IPSCs by 300 nM strychnine in Golgi cells

Parameter	Cell number										Mean ± SD
	1	2	3	4	5	6	7	8	9	10	
Cumulative amplitude, %	−38	−100	−100	−38	−39	−84	−13	+10	+4	−13	−41 ± 40
Mean frequency, %	−38	−100	−100	−14	−17	−73	−10	+11	+6	−6	−34 ± 42
Mean amplitude, %	−11	—	—	−24	−15	−42	−3	+4	0	−7	−30 ± 39

For each cell, the spontaneous IPSCs were compared in control solution and in the presence of 300 nM strychnine. Percent changes in strychnine with respect to the control values are shown. Cumulative amplitudes were obtained by adding together all detected events during time intervals of 10 or 20 s. In cells 1–6, IPSCs were partially or totally inhibited, while no significant effect was observed in cells 7–10. Note that in the latter cells, strychnine did not reduce the mean IPSC amplitude significantly.

might explain the difference of the kinetics of IPSCs apparent in Fig. 4*A*. This difference was not systematic (Fig. 3 *E* and *F*). Overall, glycinergic and GABAergic IPSCs could not be distinguished on the basis of their amplitude or of their kinetic properties. Out of 10 cells that were analyzed in detail, the spontaneous inhibitory activity was totally blocked by 300 nM to 1 μM strychnine in two cells and partially blocked in four cells (Table 1). Whereas the frequency of strychnine-sensitive events was always low (<1 Hz), high-frequency SR95531-sensitive activity (>1 Hz) was observed in the majority of cells. It is concluded that the SR95531-insensitive, strychnine-sensitive IPSCs reflect the spontaneous activity of glycinergic inhibitory inputs onto Golgi cells.

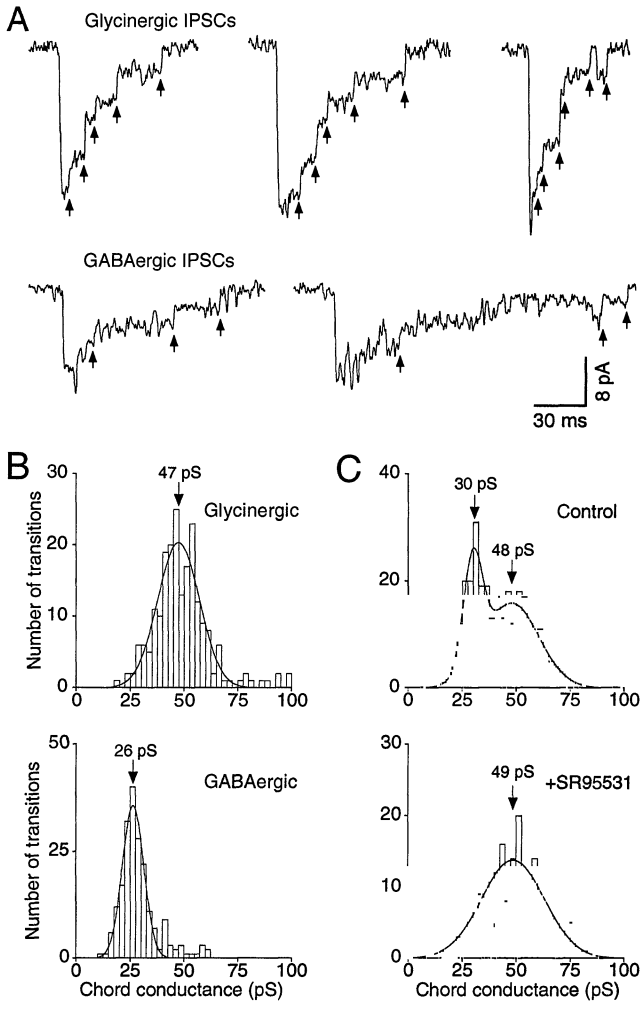

FIG. 4. Current steps in IPSCs from small Golgi cells. (*A*) Examples of current steps occurring during the decay of spontaneous IPSCs. Upper traces, glycinergic IPSCs recorded from a Golgi cell in which all IPSCs were later abolished by 300 nM strychnine (V_H = −70 mV). Lower traces, GABAergic IPSCs from a Golgi cell bathed with 3 μM strychnine (V_H = −90 mV). Part of the decay cannot be decomposed into single-channel closures. Arrows point to steps that were used to generate the histograms displayed in *B* and *C*. (*B*) Amplitude histograms of cursor-measured steps (see *Methods*) in the decay of the IPSCs. The upper and lower histograms were constructed from the data illustrated in the upper and lower traces in *A*, respectively. As the two cells were not maintained at the same holding potential, current measurements were transformed into chord conductances to allow their comparison. (*C*) Histograms constructed as in *B*, showing the distribution of the conductances in the IPSCs of another cell before (upper histogram) and after (lower histogram) addition of 30 μM SR95531. SR95531 inhibits a population of IPSCs containing small conductance events. Solid lines in *B* and *C* are Gaussian fits to the data, with the corresponding mean values.

Amplitude of the Single-Channel Current Steps in the Decay Phase of the IPSCs. The elementary conductances of the channels underlying both types of IPSCs were compared with those of the GABA-gated and glycine-gated channels described in patches (2, 30). For these recordings, small Golgi cells (compensated cell capacitance under 12 pF) were selected. In favorable cases, the falling phase of glycinergic IPSCs could be entirely described by single-channel current steps (Fig. 4*A*). The mean of the distribution estimated from these steps was 48 ± 3 pS (n = 4) (Fig. 4*B*), corresponding to the larger size of glycine-gated conductance steps (Fig. 2). By comparison, GABAergic IPSCs appeared noisier and less monotonic, so that direct measurements of channel closures were difficult. Nevertheless a tentative analysis based on the clearer transitions that were observed gave a mean conductance value close to that expected for GABA-gated channels (25 pS; n = 2). In one cell the spontaneous synaptic activity was composed of GABAergic and glycinergic events in similar proportions. In this cell, the amplitude histogram of current steps occurring during the decay of IPSCs recorded in control conditions (no SR95531, no strychnine) was best fitted by two Gaussians with means of 30 pS and 48 pS (Fig. 4*C*). After addition of 30 μM SR95531, the amplitude histogram of the steps in the remaining IPSCs was described by a single Gaussian curve with a mean of 49 pS. These results confirm that the SR95531-sensitive IPSCs, containing small current steps, are GABAergic, while the strychnine-sensitive IPSCs, containing large current steps, are glycinergic.

DISCUSSION

The results demonstrate the presence of glycinergic synaptic currents in cerebellar Golgi cells, based on three lines of evidence.

First, glycine activates a Cl-selective membrane current. This current is blocked by nanomolar concentrations of strychnine, indicating that it is linked to glycine-gated receptors. The presence of glycine receptors in Golgi cells is consistent with immunohistochemistry data. By using monoclonal antibodies against gephyrin, a glycine receptor-associated protein, Araki *et al.* (11) found immunoreactivity in dendrites of the molecular layer of the cerebellar cortex. They interpreted these dendrites as Purkinje cell dendrites, but some of them may well

be Golgi cell dendrites. Similarly, van den Pol and Gorcs (7) described glycine immunoreactive fibers, which "appeared to run along dendrites stretching between the granular layer and the outer edge of the cerebellar cortex." Such dendrites can only belong to Golgi cells.

The second line of evidence uses the $GABA_A$ inhibitor SR95531 and the glycine inhibitor strychnine to distinguish between GABA-activated and glycine-activated currents. A subpopulation of spontaneous synaptic currents were insensitive to SR95531 at concentrations saturating the GABA receptors (30 μM) and were blocked by low concentrations (300 nM) of strychnine. These pharmacological data suggest that strychnine-sensitive, SR95531-insensitive synaptic currents are mediated by glycine-activated receptors. They do not rule out, however, alternative explanations. Synaptic receptors could have pharmacological properties different from those of somatic receptors examined in outside-out patches. Alternatively strychnine could act indirectly on the synaptic activity recorded in Golgi cells by modulating a polysynaptic network in which glycinergic inhibition is essential to maintain some degree of activity.

A third, more direct support for the hypothesis that the strychnine-sensitive synaptic input was indeed glycinergic was derived from the comparison of the conductance states of the single channels underlying IPSCs with the conductance states of single channels activated by GABA and glycine in membrane patches. In outside-out patches excised from Golgi cell somata, amplitude histograms of the outward current steps during both GABA and glycine applications were clearly multimodal, but the chord conductances corresponding to the most frequent transitions were very different: 25 pS for GABA and 47 pS for glycine. Very similar values were derived from the analysis of the decay of IPSCs: 25 pS for the SR95531-sensitive events and 50 pS for the strychnine-sensitive events. It is concluded that strychnine-sensitive IPSCs result from the opening of glycine-gated channels activated by a glycinergic input onto Golgi cells.

In the only electrophysiological study of the Golgi cell to date, using intracellular recording, Midtgaard (31) concluded that the spontaneous IPSPs were GABAergic. This discrepancy with the present work could be due to species difference (turtle vs. rat) or to the rather low relative occurrence of glycinergic IPSCs compared to GABAergic IPSCs.

Spontaneous glycinergic IPSCs were observed several hours after preparing the slices. It seems unlikely that cut axon terminals could fire spontaneously over such a long period of time, suggesting that the presynaptic glycinergic neurons are located in the cerebellar cortex. All major classes of cerebellar inhibitory neurons (stellate, basket, Purkinje, and Golgi cells) have been shown to be GABAergic. Of the four cell types, only the last one is likely to include glycinergic neurons. Golgi cells accumulate [^{3}H]glycine (10), and they contain high concentrations of glycine at putative release sites in the axon terminals presynaptic to granule cell dendrites (8). Nevertheless Golgi cells are not likely to be the presynaptic cells responsible for the glycinergic input described in this study for several reasons. (*i*) No interconnection between Golgi cells has been demonstrated. (*ii*) In the present work, it was easy to trigger a retrograde action potential in Golgi cells by electrical stimulation in the granular layer surrounding the cell body, but it was very difficult to evoke glycinergic IPSPs by the same type of stimulation. (*iii*) Glycine receptor immunoreactivity is detected in synaptic spots in the molecular layer (7) where Triller *et al.* (32) have demonstrated at the ultrastructural level the clustering of glycine receptors at postsynaptic sites, while the axon of Golgi cells is confined to the granular layer.

A good candidate for the role of glycinergic interneuron is the Lugaro cell whose function and synaptic connections have not yet been elucidated (24). The cell bodies of these neurons lie in the granular layer just below the layer of Purkinje cells. They may therefore have been pooled with Golgi cells in studies of glycine uptake and glycine-like immunoreactivity. The axons of these cells descend into the granular layer (sometimes as far as the white matter) and then turn upward toward the surface of the folium. During its ascent, it could synapse in any part of the cerebellar cortex. Lainé *et al.* (33) have shown that Lugaro cells are already differentiated, with a developed axon, at the end of the first postnatal week.

I would like to thank P. Ascher and I. Llano for enthusiastic support and helpful discussions throughout this project. I also thank B. Barbour, A. Marty, and H. Gerschenfeld for critical reading of the manuscript. This work was supported by the Centre National de la Recherche Scientifique (Unité de Recherche Associée 295), the Université Pierre et Marie Curie, and the Human Frontier Research Program.

1. Aprison, M. H., Shank, R. P., Davidoff, R. & Werman, R. (1968) *Life Sci.* **7,** 583–590.
2. Takahashi, T. & Momiyama, A. (1991) *Neuron* **7,** 965–969.
3. Gold, M. R. & Martin, A. R. (1983) *J. Physiol. (London)* **342,** 85–98.
4. Korn, H. & Faber, D. S. (1990) in *Glycine Neurotransmission*, eds. Ottersen, O. P. & Storm-Mathisen, J. (Wiley, Chichester, U.K.), pp. 139–170.
5. Pourcho, R. G. & Goebel, D. J. (1990) in *Glycine Neurotransmission*, eds. Ottersen, O. P. & Storm-Mathisen, J. (Wiley, Chichester, U.K.), pp. 355–390.
6. Cortés, R. & Palacios, J. M. (1990) in *Glycine Neurotransmission*, eds. Ottersen, O. P. & Storm-Mathisen, J. (Wiley, Chichester, U.K.), pp. 239–264.
7. van den Pol, A. N. & Gorcs, T. (1988) *J. Neurosci.* **8,** 472–492.
8. Ottersen, O. P., Storm-Mathisen, J. & Somogyi, P. (1988) *Brain Res.* **450,** 342–353.
9. Pourcho, R. G., Goebel, D. J., Jojich, L. & Hazlett, J. C. (1992) *Neuroscience* **46,** 643–656.
10. Wilkin, G. P., Csillag, A., Balázs, R., Kingsbury, A. E., Wilson, J. E. & Johnson, A. L. (1981) *Brain Res.* **216,** 11–33.
11. Araki, T., Yamano, M., Murakami, T., Wanaka, A., Betz, H. & Tohyama, M. (1988) *Neuroscience* **25,** 613–624.
12. Grenningloh, G., Pribilla, J., Prior, P., Multhaup, G., Beyreuther, K., Taleb, O. & Betz, H. (1990) *Neuron* **4,** 963–970.
13. Kuhse, J., Schmieden, V. & Betz, H. (1990) *Neuron* **5,** 867–873.
14. Malosio, M.-L., Marquèze-Pouey, B., Kuhse, J. & Betz, H. (1991) *EMBO J.* **10,** 2401–2409.
15. Akaike, N. & Kaneda, M. (1989) *J. Neurophysiol.* **62,** 1400–1409.
16. Krishtal, O. A., Osipchuk, Y. V. & Vrublevsky, S. V. (1988) *Neurosci. Lett.* **84,** 271–276.
17. Trombley, P. Q. & Shepherd, G. M. (1994) *J. Neurophysiol.* **71,** 761–767.
18. Johnson, J. W. & Ascher, P. (1987) *Nature (London)* **325,** 529–531.
19. Ito, S. & Cherubini, E. (1991) *J. Physiol. (London)* **440,** 67–83.
20. Kaneda, M., Farrant, M. & Cull-Candy, S. G. (1994) *J. Physiol. (London)*, in press.
21. Llinás, R. & Sugimori, M. (1980) *J. Physiol. (London)* **305,** 197–213.
22. Edwards, F. A., Konnerth, A., Sakmann, B. & Takahashi, T. (1989) *Pflügers Arch.* **414,** 600–612.
23. Llano, I., Marty, A., Armstrong, C. M. & Konnerth, A. (1991) *J. Physiol. (London)* **434,** 183–213.
24. Palay, S. L. & Chan-Palay, V. (1974) *Cerebellar Cortex: Cytology and Organization* (Springer, Berlin).
25. Bormann, J., Hamill, O. P. & Sakmann, B. (1987) *J. Physiol. (London)* **385,** 243–286.
26. Betz, H. & Becker, C.-M. (1988) *Neurochem. Int.* **13,** 137–146.
27. Hamann, M., Désarménien, M., Desaulles, E., Bader, M. F. & Feltz, P. (1988) *Brain Res.* **442,** 287–296.
28. Twyman, R. E. & MacDonald, R. L. (1991) *J. Physiol. (London)* **435,** 303–331.
29. McNiven, A. I. & Martin, A. R. (1993) *J. Neurophysiol.* **69,** 860–867.
30. Takahashi, T., Momiyama, A., Hirai, K., Hishinuma, F. & Akagi, H. (1992) *Neuron* **9,** 1155–1161.
31. Midtgaard, J. (1992) *J. Physiol. (London)* **457,** 329–354.
32. Triller, A., Cluzeaud, F. & Korn, H. (1987) *J. Cell Biol.* **104,** 947–956.
33. Lainé, J., Axelrad, H. & Rahbi, N. (1992) *Neurosci. Lett.* **145,** 225–228.